

Complete Wetting of a Rough Surface: An X-Ray Study

I. M. Tidswell, T. A. Rabedeau, P. S. Pershan, and S. D. Kosowsky

Department of Physics and Division of Applied Sciences, Harvard University, Cambridge, Massachusetts 02138

(Received 13 February 1991)

The evolution of the surface structure of a wetting film on a rough surface as a function of the film thickness has been studied by x-ray specular reflection and surface diffuse scattering. For thin films ($\lesssim 60$ Å) the liquid surface is characterized by static undulations induced by the roughness of the substrate; however, with increasing film thickness the structure is dominated by thermally induced capillary waves. The data are quantitatively described by a model with exclusively van der Waals liquid-substrate interactions.

PACS numbers: 68.45.Gd, 68.15.+e, 68.55.Jk

Wetting thermodynamics figure prominently in a diverse collection of surface and interface phenomena¹ such as surface melting,² thin-film growth,³ and droplet spreading.⁴ While theoretically both short- and long-range forces play crucial roles in the thermodynamics of wetting, experimental investigations of the relative importance of these forces using macroscopic probes, such as contact-angle measurement, have been hampered by surface inhomogeneities such as substrate roughness and chemical heterogeneity. Despite recent experimental studies using microscopic probes,^{5,6} theoretical predictions for the influence of surface inhomogeneities on wetting films⁷ remain largely untested.

In this Letter we report the first characterization of the thickness dependence of the liquid-vapor interface structure for a thin film completely wetting a microscopically rough surface. X-ray specular reflectivity and surface diffuse scattering were measured for a silicon flat that was wet by the vapor of cyclohexane. The data are described by a model in which the only sample-dependent physical parameters are the surface tension of the bulk cyclohexane and the strength of the van der Waals interactions. For in-plane length scales of the order of 10^2 – 10^4 Å, the thinnest films are constrained by the substrate field to follow the height variations of the substrate-liquid interface; for thicker films this effect becomes weaker and the roughness of the free film surface is dominated by thermally induced capillary waves.

X-ray measurements were made at the National Synchrotron Light Source (NSLS) on beam line X16B with $k = 2\pi/\lambda = 3.714$ Å⁻¹. The incident beam was reflected from a vertically focusing mirror and an 11° asymmetrically cut Ge(111) crystal, bent to focus the beam in the horizontal plane. The approximate angular spread of the incident beam was $\Delta\alpha \approx 0.4$ mrad in the vertical scattering plane and $\Delta\Phi \sim 2$ mrad perpendicular to the scattering plane. The spectrometer utilized a two-slit detector arm that accepted ≈ 1.5 mrad in the vertical and the entire incident beam in the horizontal.

The substrates, polished Si(100) wafers coated with a native oxide film, were cleaned in a strongly oxidizing

solution to remove organic surface contaminants. The wafer was mounted horizontally against a thermoelectric device with the wafer adsorption surface facing downwards and placed in the x-ray cell 3 cm above a reservoir of approximately 5 cm³ of cyclohexane. The cell was flushed with helium before being sealed. The x-ray cell consisted of a two-stage temperature-controlled chamber with a gold-coated inner cell maintained at a temperature of 303 K with typical short-time stability of < 1 mK/(1 h) and long-time drifts of < 5 mK/(10 h). After sealing, the cyclohexane vapor saturated the cell atmosphere, wetting the substrate by vapor transport from the liquid reservoir. The wetting film thickness was controlled by differentially heating the substrate relative to the liquid reservoir by a temperature ΔT between 0 (> 100 Å film) and 0.7 K (≈ 15 Å). The differential temperature ΔT for a given thermoelectric current was calibrated before and after the x-ray measurements.

The thickness of the wetting film was measured using specular reflectivity to observe interference between reflections from the vapor-liquid and liquid-substrate interfaces.^{6,8} Typical specular reflectivity scans are shown in Figs. 1(a)–1(c) as solid symbols, together with fits with the reflectivity using a three-layer model in which the layers represent the cyclohexane, the native oxide, and the semi-infinite silicon substrate. The high quality of the fits allowed the wetting film thickness to be determined with an accuracy of ± 1.0 Å. The solid circles in Fig. 1(d) show the variation of wetting film thickness l with ΔT for these measurements. The width of the liquid-vapor interface, as measured by specular reflectivity, was approximately constant over the range of film thicknesses measured, falling in the range 3.5–3.9 Å. Dry-substrate specular reflectivity data indicate that the native oxide film is 15.8 ± 0.6 Å thick and the oxide-air interface has a 4.1 ± 0.2 -Å rms width.

Perturbations of the cyclohexane liquid surface away from an ideally flat and smooth interface were probed by measurement of the off-specular surface diffuse scattering.^{9,10} Defining z to lie along the surface normal and x in the scattering plane, radial scans of the diffuse scatter-

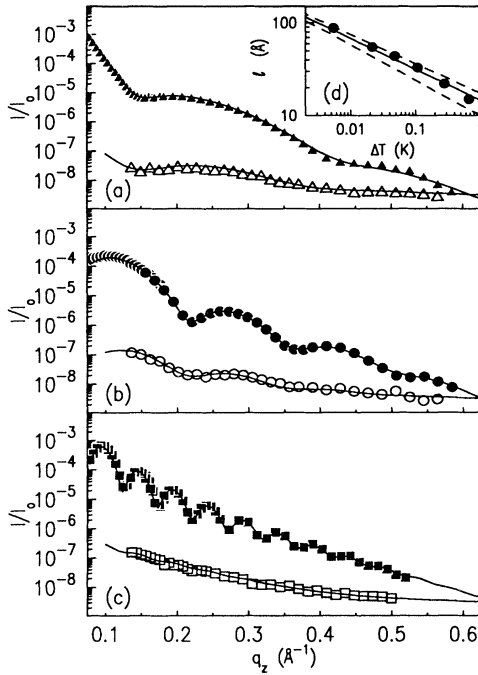


FIG. 1. Specular [solid symbols, (a)–(c)] and off-specular [$q_x/q_z=0.0026$, open symbols, (a)–(c)] scattering from substrates coated with three different thickness of cyclohexane film: (a) 22.1-Å film ($\Delta T=500$ mK), (b) 43.6-Å film ($\Delta T=100$ mK), (c) 128.1-Å film ($\Delta T \approx 0$ mK). The variation of the film thickness l with ΔT is shown in (d) together with the solid line which represents the fit described in the text; the dashed lines represent the range of l vs ΔT scaling calculated from published Hamaker constants.

ing were taken along the direction $q_x=0.0026q_z$ [Figs. 1(a)–1(c), open symbols], with $q_z=k[\sin(\alpha)+\sin(\beta)]$ and $q_x=k[\cos(\beta)-\cos(\alpha)]$, where α and β are the incident and scattered angles measured with respect to the surface plane. The diffuse scattering was also measured as a function of q_x for fixed q_z (Fig. 2).

The important feature of Figs. 1(a)–1(c) is the oscillations in the diffuse scattering for thin cyclohexane films ($\lesssim 60$ Å). These oscillations, resulting from interference

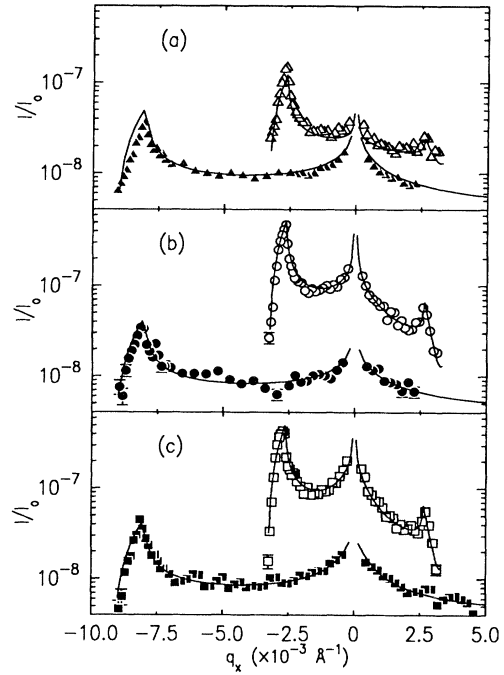


FIG. 2. Transverse (sample rocking) scans of the same three cyclohexane films as shown in Figs. 1(a)–1(c). The open symbols were measured at $q_z=0.1558$ Å⁻¹; the solid symbols were measured at $q_z=0.2597$ Å⁻¹. The latter data were multiplied by 0.5 for clarity. The solid lines are derived from best fits to the complete data set, as described in the text.

between diffuse scattering from liquid-vapor and substrate-liquid interfaces, indicate that the interfaces are correlated and that the liquid surface structure is controlled by the substrate interactions. The oscillations are *not* present for thicker films, indicating that diffuse scattering from the liquid-vapor and substrate-liquid interfaces are incoherent. This means that for thicker films the structure of the liquid-vapor interface is dominated by the liquid surface tension. Scattering from capillary waves on a thick film results in the enhanced scattering at small $|q_x|$ apparent in Fig. 2(c).

We model the measured diffuse scattering spectrum from an incident beam, intensity I_0 , as

$$I_D(\mathbf{q}) = \frac{I_0}{\alpha \Delta \alpha} \left(\frac{r_e}{k} \right)^2 \int d^3q \left\{ \frac{f(\alpha)f(\beta)}{q_z} e^{-\sigma^2 q_z^2} [S_D(\mathbf{q}) |(\rho_S - \rho_L) + \rho_L \chi(\mathbf{q}) e^{iq_z l}|^2 + S_{\text{cap}}(\mathbf{q})] \right\}, \quad (1)$$

where ρ_S and ρ_L are the electron densities of the substrate and liquid film, respectively, and the integral is over the spectrometer resolution volume. The function $f(\alpha) = (2\alpha/\theta_c)^2 [R_F(\alpha)]^{1/2}$ represents the Fresnel surface scattering enhancement factor,^{9,10} where θ_c is the critical angle for total reflection and R_F is the Fresnel reflectivity from an ideally smooth sharp surface. The term $f(\alpha)f(\beta)$ is responsible for the peaks at nonzero q_x in Fig. 2. The Gaussian term represents a “Debye-Waller”-like attenuation of the scattering, where $\sigma=4.1$

Å is the measured rms roughness of the dry substrate as noted above.¹¹ This model neglects the small (about 5%) electron-density difference between the silicon and silicon-oxide layers.

The function S_D represents the scattering from the dry-substrate surface and has the empirical form $S_D(\mathbf{q}) = S_d |q_{\parallel}|^{-\nu}$, where $q_{\parallel} = (q_x^2 + q_y^2)^{1/2}$ and ν and S_d are constants to be determined. Modeling the data from one off-specular radial scan and four transverse scans of the

dry substrate ($0.15 \leq q_z \leq 0.33 \text{ \AA}^{-1}$) in the region $|\alpha - \beta| \geq 0.2^\circ$ (i.e., away from the specular condition) with this form gave $\nu = 1.49 \pm 0.10$ with $\chi^2 = 1.8$ for the 156 data points. The empirically determined values of ν and S_d were used in modeling the wetting film.

The term $[(\rho_S - \rho_L) + \rho_L \chi(\mathbf{q}) e^{iq_z l}]^2$ represents scattering from the substrate-liquid interface and the correlated portion of the scattering from the liquid-vapor surface. The function $\chi(\mathbf{q})$ is the "susceptibility" of the liquid-vapor surface to the substrate-liquid interface structure. The form^{7(a)}

$$\chi(\mathbf{q}) = a^2 / (|q_{\parallel}|^2 l^4 + a^2) \quad (2)$$

is derived by considering a molecular van der Waals interaction ($\epsilon = -a_{ij} r^{-6}$) within the Derjaguin approximation.¹² The strength of the van der Waals interactions is contained in the "characteristic length" $a = (A_{\text{eff}}/2\pi\gamma)^{1/2}$, where γ is the liquid-vapor surface tension and A_{eff} is the effective Hamaker constant. For a homogeneous substrate, $A_{\text{eff}} = A_{LS} - A_{LL}$, with L referring to the liquid and S the substrate, whereas for a solid substrate coated with a solid film F of mean thickness d , $A_{\text{eff}} \approx A_{FL} - A_{LL} + (A_{SL} - A_{FL})(1 + d/l)^{-3}$. Here we use the definition of the Hamaker constant $A_{ij} = \pi^2 n_i n_j \times a_{ij}$, where $n_{i,j}$ is the molecular number density, and the approximation $a_{ij} = (a_{ii} a_{jj})^{1/2}$.

The function S_{cap} describes the uncorrelated scattering from capillary waves at the liquid-vapor surface. Assuming that the substrate force field does not vary significantly over the amplitude of the capillary waves, the spectrum of these waves is very similar to the spectrum for bulk liquid surfaces¹⁰ with the gravitational cutoff $k_g^2 = \rho g / \gamma$ replaced by a much larger van der Waals cutoff $k_{\text{vW}}^2 = a^2 / l^4$:

$$S_{\text{cap}}(\mathbf{q}) = \frac{k_B T}{\gamma} \frac{l^4}{|q_{\parallel}|^2 l^4 + a^2}, \quad (3)$$

where γ is the liquid surface tension (for cyclohexane $\gamma = 25.5 \text{ erg cm}^{-2}$). An additional term describing the background scattering from the bulk vapor and bulk substrate was also included.

Relative to the length scale over which the integrand of Eq. (1) varies, the spectrometer resolution used for the diffuse scattering measurements was quite narrow in the scattering plane and coarse perpendicular to the scattering plane (q_y). Consequently, after explicit integration over q_y , Eq. (1) was approximated by the product of the integrand and the scattering-plane resolution $[\Delta\alpha\Delta\beta k^2 \sin(2\theta)]$. The complete data set, a representative fraction of which is shown in Figs. 1(a)–1(c) and 2, consists of two off-specular radial scans and three transverse scans at different q_z taken for each of seven film thicknesses, with a total of 1345 points. An excellent description of the diffuse scattering data was obtained by using $A_{\text{eff}} = 5.9 \times 10^{-13} \text{ erg}$ (see below) in Eqs. (1)–(3) and fitting only the bulk diffuse background intensity;

this is demonstrated by the fit to the off-specular data shown as the line in Figs. 1(a)–1(c) and 2, corresponding to a χ^2 of 2.2.

The effective Hamaker constant used above was extracted from the data for l vs ΔT using the approximation $-(\partial\Delta\mu/\partial T)_p \Delta T = A_{\text{eff}} / (6\pi n_L) l^{-3}$, where $\Delta\mu$ is the difference of the chemical potential between the bulk liquid and vapor at these temperatures.¹³ Representing the substrate as a homogeneous media (i.e., ignoring the difference in Hamaker constants between the silicon substrate and silicon-oxide film) and using the approximation that $-(\partial\Delta\mu/\partial T)_p \approx q/T$, where q is the latent heat of vaporization per molecule ($q \approx 5.4 \times 10^{-13} \text{ erg}$), the best fit for A_{eff} is shown by the solid line in Fig. 1(d). The fit yields the effective Hamaker constant between the substrate and the cyclohexane, $A_{\text{eff}} = (5.9 \pm 2.0) \times 10^{-13} \text{ erg}$, this value being used above to describe the surface diffuse scattering. A more complete description of the system would include the different Hamaker constants of the silicon substrate and silicon-oxide films, leading to an l dependence for A_{eff} ; unfortunately, the data for l vs ΔT are not sufficiently precise to extract this dependence.

An independent estimate of A_{eff} can be obtained from previously published experimental and theoretical values.¹⁴ While the reported values for the Hamaker constants of silicon and cyclohexane are relatively well characterized, the estimates for silicon oxide vary by almost an order of magnitude from study to study.¹⁴ The dashed lines in the inset of Fig. 1 show the range of l vs ΔT deduced from using the extremum values of the silicon-oxide Hamaker constant $[(8.5\text{--}50) \times 10^{-13} \text{ erg}]$ and reasonable estimates for silicon and cyclohexane (24×10^{-13} and $4.6 \times 10^{-13} \text{ erg}$, respectively).¹⁴ These lines lie on either side of both the experimental data and the fitted line, giving confidence that the values for the Hamaker constant determined from the data are physically reasonable.

In summary, for film thicknesses of 15–130 \AA and surface roughness wave vectors of 10^{-2} – 10^{-4} \AA^{-1} , we have demonstrated that both the temperature variation of the mean thickness and the surface profile of nonpolar liquid adsorbed on a microscopically rough substrate can be fully described in terms of a simple application of the van der Waals interaction. In agreement with theoretically predicted^{7(a)} but previously unobserved behavior, we find that for very thin films the substrate van der Waals interactions constrain the liquid surface to follow the static undulations of the substrate, whereas for thicker films, the liquid surface structure is dominated by thermally induced capillary waves.

We wish to thank M. Deutsch for useful discussions and a critical reading of the manuscript, and J. P. Folkers and G. M. Whitesides for useful discussions. The assistance of the X16B beam line staff is also acknowledged. This work was supported by the National Science Foundation through Grant No. NSF DMR-89-

20490. Research carried out at the NSLS, Brookhaven National Laboratory, is supported by the Department of Energy, Materials Sciences, and Division of Chemical Sciences under Contract No. DE-AC02-76CH00016. X16B is supported by AT&T Bell Laboratories.

¹For complete reviews, see P. G. de Gennes, *Rev. Mod. Phys.* **57**, 827 (1985), and S. Dietrich, in *Phase Transitions and Critical Phenomena*, edited by C. Domb and J. L. Lebowitz (Academic, New York, 1988), Vol. 12.

²J. W. M. Frenken and J. F. van der Veen, *Phys. Rev. Lett.* **54**, 134 (1985).

³M. Copel, M. C. Reuter, E. Kaxiras, and R. M. Tromp, *Phys. Rev. Lett.* **63**, 632 (1989); H. S. Youn and G. B. Hess, *Phys. Rev. Lett.* **64**, 918 (1990).

⁴F. Heslot, A. M. Cazabat, P. Levinson, and N. Fraysse, *Phys. Rev. Lett.* **65**, 599 (1990).

⁵P. Pfeifer, Y. J. Wu, M. W. Cole, and J. Krim, *Phys. Rev. Lett.* **62**, 1997 (1989).

⁶S. Garoff, E. B. Sirota, S. K. Sinha, and H. B. Stanley, *J. Chem. Phys.* **90**, 7505 (1989).

^{7(a)}D. Andelman, J.-F. Joanny, and M. O. Robbins, *Europhys. Lett.* **7**, 731 (1988); M. O. Robbins, D. Andelman, and J.-F. Joanny, *Phys. Rev. A* **43**, 4344 (1991); (b) M. Kardar and J. O. Indekeu, *Europhys. Lett.* **12**, 161 (1990).

⁸J. Als-Nielsen, *Physica (Amsterdam)* **140A**, 376 (1986).

⁹S. K. Sinha, E. B. Sirota, S. Garoff, and H. B. Stanley, *Phys. Rev. B* **38**, 2297 (1988); M. K. Sanyal, S. K. Sinha, K. G. Huang, and B. M. Ocko, *Phys. Rev. Lett.* **66**, 628 (1991).

¹⁰A. Braslau, M. Deutsch, P. S. Pershan, A. H. Weiss, and J. Als-Nielsen, *Phys. Rev. Lett.* **54**, 114 (1985); D. K. Schwartz, M. L. Schlossman, E. H. Kawamoto, G. J. Kellogg, P. S. Pershan, and B. M. Ocko, *Phys. Rev. A* **41**, 5687 (1990).

¹¹More accurately, a separate σ should be assigned to each interface. For our data, the small error introduced by the difference between the substrate-liquid and liquid-vapor interface widths is negligible.

¹²B. V. Derjaguin, N. V. Churaev, and V. M. Muller, *Surface Forces* (Consultants Bureau, New York, 1987).

¹³Omitted from this expression is a term representing the reduction in surface entropy due to the proximity of the substrate, see J. Frenkel, *Kinetic Theory of Liquids* (Dover, New York, 1955), Chap. 6; however, these contributions in this system are small relative to the other terms and in any case have the same l dependence as the surface energy.

¹⁴J. Visser, *Adv. Colloid Interface Sci.* **3**, 331 (1972).